

PACS numbers: 42.55.Wd; 42.65.Sf
DOI: 10.1070/QE2014v044n04ABEH015363

Cross modulation instability in normal-dispersion fibre lasers and amplifiers

I.O. Zolotovskii, D.A. Korobko, V.A. Lapin

Abstract. **This paper examines instability resulting from cross phase modulation interaction between signal and pump waves in normal-dispersion fibre lasers and amplifiers. From analysis of the dispersion relation for the wave vector of small harmonic perturbations, we derive dynamic spectral characteristics of the modulation gain coefficient. Its dependence on the group velocity difference between signal and pump waves is investigated. Analytical results are compared to numerical simulation data. We discuss how the general relationships obtained in this study can be used in practical applications.**

Keywords: *fibre lasers and amplifiers, modulation instability, cross phase modulation.*

1. Introduction

Modulation instability (MI) – growth of small harmonic perturbations of a continuous wave – is characteristic of many nonlinear systems that support the propagation of localised waves and is related to an interplay between nonlinearity and dispersion [1, 2]. In fibre optics, MI was first predicted theoretically and demonstrated experimentally for anomalous-dispersion fibres, in which a continuous modulated wave was observed to convert into a pulse train [3, 4]. In such instances, the instability responsible for perturbation growth originates from interaction between the nonlinear self-phase modulation (SPM) and anomalous dispersion of a modulated wave. Subsequently, MI in fibre optics has been the subject of extensive studies. Here, we mention only recent reports, in particular those concerned with studies of MI in fibre amplifiers [5] and anomalous dispersion decreasing fibres [6] and with the effect of higher order nonlinearities (self-steepening parameters and delayed nonlinear response of a fibre) on MI [7, 8]. Intense research interest in MI is aroused not only by its general fundamental importance but also by its possible applications in some areas of nonlinear fibre optics: generation of high-frequency trains of short pulses [9] and creation of broadband light sources [10, 11].

Of special note is instability arising when two or more waves simultaneously propagate through a fibre. Interaction between them results in an additional factor: nonlinear cross phase modulation (XPM), which is also capable of increasing harmonic perturbations, in particular in the normal-dispersion region of interacting propagating waves in the case where 'conventional' MI does not develop [12, 13]. From an applied point of view, an important issue is to study the MI induced by the cross modulation interaction between a pump wave and signal wave in Raman fibre lasers and amplifiers [14, 15]. To our knowledge, no theoretical studies have examined the development dynamics of cross modulation instability in the case of signal amplification with allowance for pump depletion. This issue is addressed in the present study, with a great deal of attention paid to the effect of the group velocity difference between signal and pump waves on the development of MI. This parameter determines many aspects of the development of cross modulation instability. In particular, no such instability develops at a large group velocity difference, e.g. in the case of counterpropagating pump and signal waves. This has been demonstrated experimentally [15, 16]. Knowledge of the modulation gain as a function of group velocity difference offers an additional possibility of controlling the MI process, e.g. by varying the pump frequency and, accordingly, the pump–signal group velocity difference. Strictly speaking, the present results are applicable not only to Raman amplifiers but also to all fibre amplifiers in which the signal and pump group velocities and, hence, frequencies differ relatively little. The general relationships identified here can be used not only in applications where MI is necessary (e.g. in designing fibre oscillators for new frequency ranges) but also when parasitic MI should be suppressed.

2. Basic relations

Consider the propagation of a pump wave (carrier frequency ω_p) and signal wave (carrier frequency ω_s) in a fibre amplifier (along the z axis). Taking into account nonlinear cross modulation interaction, we can describe it by the following system of equations for the complex temporal envelopes $A_p(z,t)$ and $A_s(z,t)$ [1]:

$$\begin{aligned}
&\frac{\partial A_p}{\partial z}+\frac{1}{v_{gp}}\frac{\partial A_p}{\partial t}+\frac{i}{2}d_p\frac{\partial^2 A_p}{\partial t^2}+\frac{\alpha_p(z)}{2}A_p\\
&\quad=i\gamma_p(|A_p|^2+2|A_s|^2)A_p,\\
&\frac{\partial A_s}{\partial z}+\frac{1}{v_{gs}}\frac{\partial A_s}{\partial t}+\frac{i}{2}d_s\frac{\partial^2 A_s}{\partial t^2}+\frac{\alpha_s(z)}{2}A_s\\
&\quad=i\gamma_s(|A_s|^2+2|A_p|^2)A_s,
\end{aligned}\tag{1}$$

where $v_{gj}=\mathrm{d}\omega/\mathrm{d}\beta_j$ is the group velocity of the wave; γ_j is the nonlinearity parameter; and β_j and d_j are the propagation

I.O. Zolotovskii, D.A. Korobko, V.A. Lapin Ulyanovsk State University, ul. L. Tolstogo 42, 432017 Ulyanovsk, Russia; e-mail: rafzol.14@mail.ru, korobkotam@rambler.ru

Received 10 December 2013; revision received 31 January 2014
Kvantovaya Elektronika **44** (4) 345–352 (2014)
Translated by O.M. Tsarev

constants and group velocity dispersions of the corresponding waves. The variable coefficients $\alpha_j(z)$ quantify signal amplification and pump depletion. They can be found from a system of equations for continuous waves, $|A_p(z,t)|^2 = P_p(z)$ and $|A_s(z,t)|^2 = P_s(z)$, which describes pump-to-signal power conversion and is generally valid not only for stimulated Raman amplification but also for any three-level laser medium. In the undepleted pump approximation, neglecting the intrinsic pump and signal wave absorption, we can write this system in the form [1, 17]

$$\begin{aligned} &dP_s/dz = g_R P_s P_p, \\ &dP_p/dz = -(\omega_p/\omega_s) g_R P_s P_p. \end{aligned} \tag{2}$$

Here, g_R is pump efficiency. In the case of stimulated Raman scattering (SRS), it is the Raman gain coefficient, related to the spontaneous Raman scattering cross section. For an arbitrary three-level laser system (e.g. the erbium-doped fibre amplifier), it can be expressed as

$$g_R = \frac{N\sigma_s\sigma_p}{(\eta_0 + 1/\tau_{21})\hbar\omega_p S_{eff}},$$

where N is the active centre concentration; τ_{21} is the metastable-level lifetime, which determines the spontaneous transition rate; σ_p is the pump absorption cross section; σ_s is the emission cross section at the signal wavelength; S_{eff} is the effective mode area; and η_0 is the net stimulated transition rate for pump absorption and signal emission. In a steady state, if the active centre concentration is, on average, constant along the fibre length, then so is the transition rate, $\eta_0(z) = \text{const}$, which is analogous to the conservation of the number of photons in SRS. In the approximation under consideration (with no intrinsic absorption) and with spontaneous luminescence neglected, this leads to the conservation of total power (with allowance for frequency conversion):

$$P_p + (\omega_p/\omega_s)P_s = P_0 = \text{const}.$$

Using the notations $\chi = \omega_s P_{p0}/(\omega_p P_{s0})$ and $\theta = g_R(1+\chi)P_{p0}\omega_p/\omega_s$, where $P_{p0} = |A_p(0,t)|^2$ and $P_{s0} = |A_s(0,t)|^2$ are the initial pump and signal powers, we obtain expressions for the gain and depletion coefficients [17]:

$$\begin{aligned} &\alpha_s = -g_R P_p = -\frac{g_R P_{p0}(1+\chi)}{\chi + \exp(\theta z)}, \\ &\alpha_p = \frac{\omega_p}{\omega_s} g_R P_s = \frac{\omega_p}{\omega_s}\frac{g_R P_{s0}(1+\chi)}{\chi + \exp(\theta z)}\exp(\theta z). \end{aligned} \tag{3}$$

Substitution of

$$A_j(z,t) = B_j(z,t)\exp\left[-\frac{1}{2}\int_0^z \alpha_j(\xi)\,d\xi\right]$$

transforms (1) to a form corresponding to a system with no gain, but with variable nonlinearity coefficients, which can be found by integration:

$$\begin{aligned} &\frac{\partial B_j}{\partial z} + \frac{1}{v_{gj}}\frac{\partial B_j}{\partial t} + \frac{i}{2}d_j\frac{\partial^2 B_j}{\partial t^2} \\ &\quad = i[\tilde\gamma_{jj}(z)|B_j|^2 + 2\tilde\gamma_{j3-j}(z)|B_{3-j}|^2]B_j, \end{aligned}$$

$$\begin{aligned} &\tilde\gamma_{j1} = \gamma_j\left(\frac{\chi + \exp(\theta z)}{1+\chi}\right)^{-S},\ S = \frac{g_R P_{s0}(1+\chi)}{\theta}, \\ &\tilde\gamma_{j2} = \gamma_j\frac{1+\chi}{\chi + \exp(\theta z)}\exp\left[\frac{g_R P_{p0}(1+\chi)z}{\chi}\right]. \end{aligned} \tag{4}$$

Here and in what follows, we use the notation $p \leftrightarrow 1$, $s \leftrightarrow 2$ and $j = 1, 2$. System (4) has a steady-state solution. Note that the path length in the fibre, z, influences only the phase shift φ_j of the propagating monochromatic wave:

$$\begin{aligned} &B_j(z) = \sqrt{P_{j0}}\exp(i\varphi_j), \\ &\varphi_j = P_{j0}\int_0^z \tilde\gamma_{jj}(\xi)\,d\xi + 2P_{3-j0}\int_0^z \tilde\gamma_{j3-j}(\xi)\,d\xi, \end{aligned}$$

where P_{j0} is the light power coupled into the fibre.

Our main purpose in this study is to assess the stability of the constant steady-state solution to small perturbations. We represent the solution to (4) in the form

$$B_j(t,z) = [\sqrt{P_{j0}} + b_j(t,z)]\exp(i\varphi_j), \tag{5}$$

where $|b_j| \ll \sqrt{P_{j0}}$, and examine perturbation dynamics. Following Agrawal [12], consider harmonic wave perturbations, which can be represented in standard form:

$$b_j(z,t) = U_j\cos(Kz - \Omega t) + iV_j\sin(Kz - \Omega t), \tag{6}$$

where K is the wavenumber and Ω is the modulation frequency. We will consider a simple case of single-frequency (Ω) modulation due to a harmonic perturbation of the pump or signal wave. A perturbation of the pump wave (or signal) at a frequency $\omega_v = \omega_j - \Omega$ leads to modulation of the other wave at a perturbation frequency $\omega_{v'} = \omega_{3-j} - \Omega$. Whether the steady-state solution is stable or unstable to small perturbations, $b_j(z,t)$, is determined by the modulation wavenumber dispersion, $K(\Omega)$. When $K(\Omega)$ has an imaginary part, small perturbations grow exponentially and the steady-state solution is unstable. Substituting (5) into (4) and linearising with respect to the small parameter, we obtain the following system of equations describing the dynamics of small perturbations in the fibre:

$$\begin{aligned} &\frac{\partial b_j}{\partial z} + \frac{1}{v_{gj}}\frac{\partial b_j}{\partial t} + \frac{i}{2}d_j\frac{\partial^2 b_j}{\partial t^2} \\ &\quad = i[P_{j0}\tilde\gamma_{jj}(b_j + b_j^*) + 2\tilde\gamma_{j3-j}\sqrt{P_{j0}P_{3-j0}}(b_{3-j} + b_{3-j}^*)]. \end{aligned} \tag{7}$$

Following a standard procedure, we substitute perturbation (6) into these equations and obtain a system of equations in U_j and V_j. Equating the determinant of this system to zero, we find a dispersion relation between parameters of the perturbation and those of the fibre and pump wave:

$$\left[\left(K - \frac{\Omega}{v_{gp}}\right)^2 - f_p\right]\left[\left(K - \frac{\Omega}{v_{gs}}\right)^2 - f_s\right] = C_{XPM}, \tag{8}$$

where the following notations are used:

$$\begin{aligned} &f_j = \frac{d_j\Omega^2}{2}\left(\frac{d_j\Omega^2}{2} + 2\tilde\gamma_{jj}P_{j0}\right), \\ &C_{XPM} = 4\tilde\gamma_{ps}\tilde\gamma_{sp}P_{p0}P_{s0}d_p d_s\Omega^4. \end{aligned} \tag{9}$$

An important distinction from what was reported by Agrawal [12] is that these coefficients vary along the length of the amplifier and determine modulation gain dynamics. In what follows, we analyse the above dispersion relation and examine the behaviour of the modulation gain coefficient $g(\Omega) = 2\,\mathrm{Im}\,K(\Omega)$ in the signal amplification process and in relation to the group velocity difference $\delta = |1/v_{gp} - 1/v_{gs}|$.

It is worth noting that a simplified description of cross modulation interaction is possible, which neglects the group velocity difference between interacting waves. This is, of course, relevant when the interacting waves are identical or differ very little in frequency, but the frequency difference and, accordingly, group velocity difference in amplification systems are rather significant. In an inverse approach, we can neglect the term describing cross modulation by virtue of the group velocity difference between the waves. However, even though a group velocity difference restricts cross modulation interaction and eventually suppresses it, the question of modulation stability/instability of radiation in optical amplifiers with a copropagating pump and signal configuration remains open. This is particularly so in the case of Raman lasers, Raman amplifiers and other laser systems in which the pump and signal frequencies differ relatively little [14–16]. An important distinction of our approach is that we take into account the dependence of the modulation gain on the group velocity difference parameter δ.

3. Analysis of the dispersion relation and the behaviour of cross modulation instability in gain dynamics

In what follows, we will restrict our consideration to the case where both a pump wave and a signal wave propagate in the normal-dispersion regime ($d_p > 0$, $d_s > 0$), which will allow us to separately consider the instability caused by the cross modulation interaction between the pump and the signal wave in an amplifier. Recall that the nonlinear SPM of an individual wave propagating through an anomalous-dispersion medium ($d < 0$) also leads to instability, i.e. small harmonic perturbations $\pm\Omega$ at the frequency of a continuous wave of power P_0 in a fibre with a nonlinearity parameter γ are amplified [1]:

$$g(\Omega) = |d|\,\Omega\sqrt{\Omega_c^2 - \Omega^2}\,,\ \ \Omega_c^2 = 4\gamma P_0/|d|\,.$$

In what follows, we assume that, in a normal-dispersion fibre, such instability does not develop, which is generally not so in the spectral range corresponding to low positive group velocity dispersion (d) values. MI is then determined as well by the influence of fourth-order dispersion (for $d_4 < 0$). The comparatively narrow MI range near a frequency $\Omega_c = \sqrt{-12d/d_4}$ is defined by the inequalities [18]

$$d + d_4\Omega^2/12 < 0,\ \ |d + d_4\Omega^2/12|\,\Omega^2 < 4\gamma P_0.$$

This may be essential in the case of special microstructured waveguides, in which waveguide dispersion is rather high. Nevertheless, in most standard situations, i.e. at negligible or positive d_4 values and far away from the zero dispersion wavelength, our consideration is valid.

We now turn to analysing the dispersion relation (8). Its real roots describe the propagation of modulation with a spatial period $z = 2\pi/K(\Omega)$ and are of no interest. Useful information about modulation amplification is provided by conjugate complex roots, which determine the nature of the modulation gain coefficient, $g(\Omega) = 2\,\mathrm{Im}\,K(\Omega)$. (Clearly, one of the roots describes modulation attenuation, which can be neglected when there is amplification.) Since modulationally unstable solutions should meet phase matching conditions, it can be shown that the real part of these roots, $\mathrm{Re}\,K(\Omega)$, should be close to $\delta\Omega$.

The process of analytically solving (8), an equation of the fourth degree, is unwieldy and time-consuming, so further results were obtained by numerically finding its roots. Note that, for an arbitrary set of parameters converting (8) to an equation with numerical coefficients, we compared the exact analytical solution and a numerical one, which coincided to within 10^{-8}, demonstrating that the numerical method used was quite accurate.

As the first step, we investigated cross modulation instability without allowance for the dynamics of the pump and signal powers, at parameters typical of fibres with normal dispersion in the IR spectral region and at a signal to pump frequency ratio, ω_s/ω_p, near the ratio of the pump frequency to the Stokes Raman frequency in this range. To this end, at the initial length of the amplifier, $z = 0$, we considered the function $g(\Omega)$ at varied signal to pump power ratio, P_{s0}/P_{p0} (Fig. 1a). It is seen that the 'instantaneous' cross modulation gain is only appreciable under high-power pumping at com-

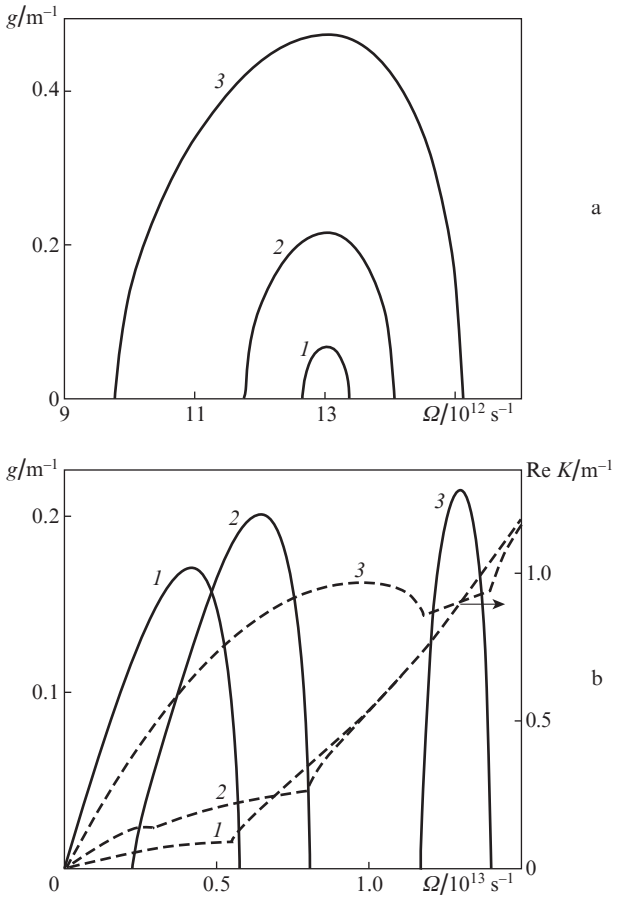

Figure 1. Modulation gain coefficient $g(\Omega)$ at $z = 0$ in an amplifier with $g_R = 0.005$ W^{-1} m^{-1}, $\gamma_1 = \gamma_2 = 0.005$ W^{-1} m^{-1}, $\omega_s/\omega_p = 0.95$, $d_p = 0.02$ ps^2 m^{-1}, $d_s = 0.01$ ps^2 m^{-1} and $P_{p0} = 25$ W (solid lines): (a) $\delta = 0.2$ ps m^{-1}, $P_{s0}/P_{p0} = (1)\,0.02$, $(2)\,0.2$, $(3)\,1$; (b) $P_{s0}/P_{p0} = 0.2$, $\delta = (1)\,0.05$, $(2)\,0.1$, $(3)\,1$ ps m^{-1}. The dashed lines show the real part of the corresponding roots $K(\Omega)$.

parable pump and signal powers. Therefore, when small signals are amplified, especially at a small Raman gain coefficient, g_R, a long length of the amplifier is needed for the onset of MI. It is worth noting that the frequency range of MI is well away from the origin, $\Omega = 0$, i.e. MI develops only in a band at relatively high frequencies. The reason for this is that, at low Ω frequencies, MI is suppressed owing to the pump–signal group velocity difference.

Figure 1b presents frequency dependences of the modulation gain at an initial length $z = 0$ and different group velocity differences, δ. As would be expected, the $g(\Omega)$ curve shifts towards the origin with decreasing δ and takes a standard shape at low δ, describing instability in the frequency range $\Omega \in [0, \Omega_c]$. As mentioned above, this behaviour can be accounted for in terms of phase matching between the signal and pump modulations. For the corresponding condition to be fulfilled at $\delta \neq 0$, the complex roots of the dispersion relation (8) should have a nonzero real part, describing the spatial shift of the growing modulation (at $\delta = 0$, the dispersion relation reduces to a biquadratic equation, and growing modulation is described by its purely imaginary roots [12, 13]). The $\mathrm{Re}\,K(\Omega)$ curves are shown in Fig. 1b by dashed lines. With increasing group velocity difference δ, the relation $\mathrm{Re}\,K(\Omega) \approx \delta\Omega$ in the instability band is satisfied more and more accurately, reducing the width of the band and shifting it to higher modulation frequencies. At a large group velocity difference, the instability band essentially 'collapses' into a narrow line and shifts to frequencies comparable to the carrier frequency ω_j, suggesting complete MI suppression.

Figure 2 shows the modulation gain coefficient g as a function of dispersion and nonlinearity parameters at a particular signal power, pump power and group velocity difference. Since the parameters d_p and d_s appear in the coefficients of the dispersion relation as the $d_j\Omega^2$ product, the position of the maximum in gain, i.e. the frequency Ω_{max} at which the imaginary part of $K(\Omega)$ has a maximum, can be expressed with good accuracy as [12]

$$\Omega_{max} = \delta(d_p d_s)^{-1/2}, \tag{10}$$

which is supported, e.g., by the data in Fig. 2. Note that, with increasing dispersion, the instability band shifts to lower frequencies, i.e., the dispersion of the fibre counterbalances the pump–signal group velocity difference. Figure 2b demonstrates that the modulation gain coefficient is a strong function of fibre nonlinearity parameters. It is worth noting in this context that the nonlinearity parameter has a weak effect on the peak gain frequency and typically increases the maximum gain and instability bandwidth.

The general relationships above refer to an 'instantaneous' modulation gain coefficient, i.e. one obtained at a particular pump power and signal power. In a real amplification system, these parameters vary constantly: the pump power is converted to the signal. As a result, the modulation gain coefficient also varies constantly. This process is illustrated by Fig. 3, which presents results of analysis of the dispersion relation (8) in terms of gain dynamics. The evolution of the modulation gain coefficient is demonstrated at different δ values, typical of silica fibres in the IR spectral region ($\lambda > 1200$ nm) at a difference between the pump and signal wavelengths $\Delta\lambda \approx 80$ nm, which roughly corresponds to the difference between the pump and Stokes signal wavelengths in this range in the case of stimulated Raman amplification [19]. The highest modulation gain and the largest spectral width of the MI range are ensured

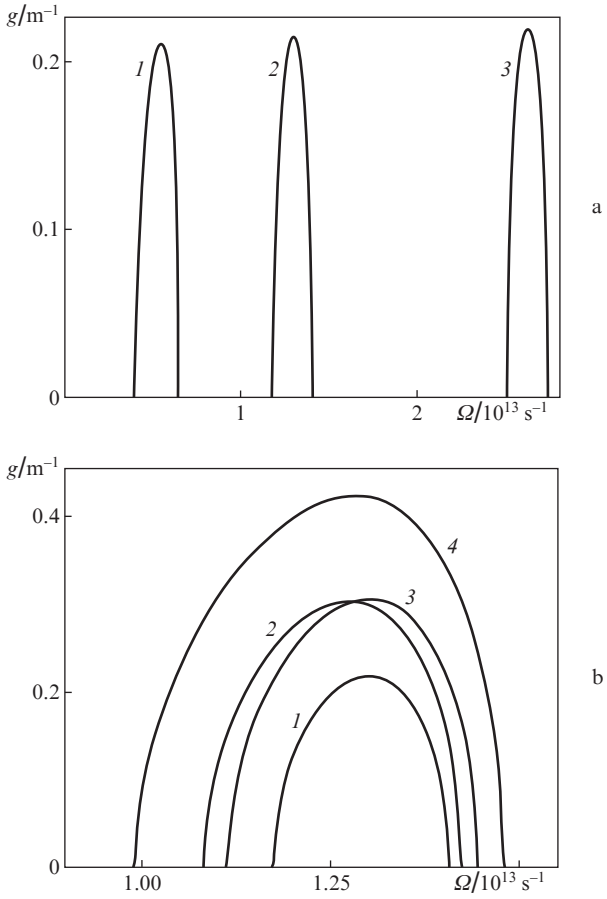

Figure 2. Modulation gain coefficient $g(\Omega)$ at $z = 0$ in an amplifier with $g_R = 0.005$ W^{-1} m^{-1}, $\omega_s/\omega_p = 0.95$, $\delta = 0.2$ ps m^{-1}, $P_{p0} = 25$ W and $P_{s0}/P_{p0} = 0.2$: (a) $\gamma_1 = \gamma_2 = 0.005$ W^{-1} m^{-1}; $d_p = (1)$ 0.04, (2) 0.02 and (3) 0.01 ps^2 m^{-1}; $d_s = (1)$ 0.03, 0.01 and 0.005 ps^2 m^{-1}; (b) $d_p = 0.02$ ps^2 m^{-1}; $d_s = 0.01$ ps^2 m^{-1}; $\gamma_1 = (1,3)$ 0.005 and $(2,4)$ 0.01 W^{-1} m^{-1}; $\gamma_2 = (1,2)$ 0.005 and $(3,4)$ 0.01 W^{-1} m^{-1}.

by the amplifier length at which the pump power is equal to the signal power (see also Fig. 4a). Further pump depletion is accompanied by a decrease in modulation gain, which is almost symmetric with respect to the point where the pump power is equal to the signal power. Note again that the spectral range of instability is broader at the minimum group velocity difference and that, with increasing group velocity difference δ, the instability bandwidth decreases markedly.

4. Numerical simulation of cross modulation instability in an amplifier

Numerical simulation was used to examine the cross modulation process in a normal group velocity dispersion amplifier. Using the standard split-step Fourier method, we modelled the system of equations [1]

$$\begin{aligned}
&\frac{\partial A_p}{\partial z} + \frac{i}{2} d_p \frac{\partial^2 A_p}{\partial t^2} + \frac{\omega_p}{\omega_s} \frac{g_R |A_s|^2}{2} A_p \\
&\quad = i\gamma_p (|A_p|^2 + 2|A_s|^2) A_p, \\
&\frac{\partial A_s}{\partial z} + \frac{1}{\delta} \frac{\partial A_s}{\partial t} + \frac{i}{2} d_s \frac{\partial^2 A_s}{\partial t^2} - \frac{g_R |A_p|^2}{2} A_s \\
&\quad = i\gamma_s (|A_s|^2 + 2|A_p|^2) A_s.
\end{aligned} \tag{11}$$

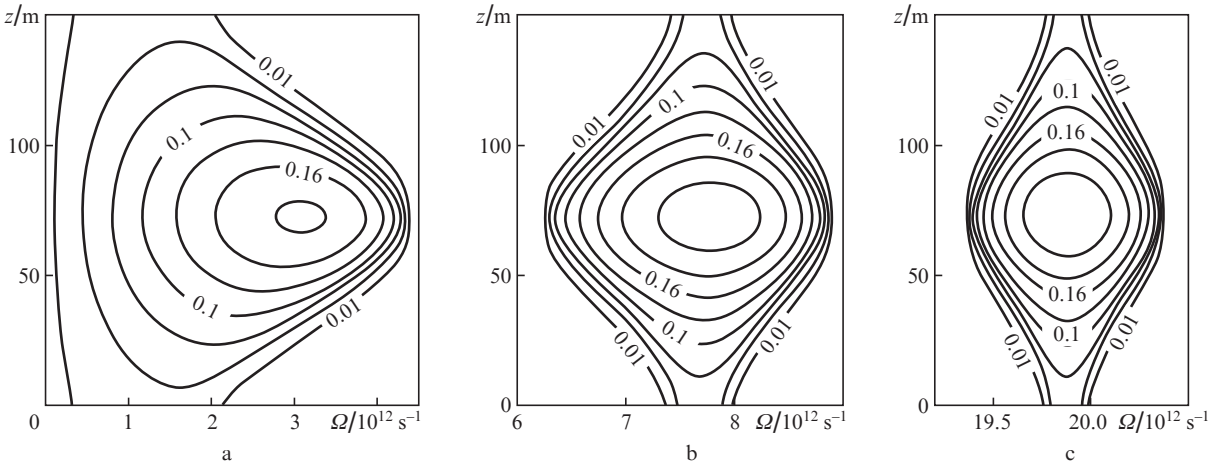

Figure 3. Frequency dependences of the cross modulation gain coefficient for signal propagation in an amplifier with $\omega_s/\omega_p = 0.95$, $g_R = 0.0025$ W^{-1} m^{-1}, $P_{p0} = 25$ W, $P_{s0} = 0.25$ W, $d_p = 0.03$ ps^2 m^{-1}, $d_s = 0.02$ ps^2 m^{-1}, $\gamma_p = \gamma_s = 0.005$ W^{-1} m^{-1} and δ = (a) 0.05, (b) 0.2 and (c) 0.5 ps m^{-1}. The contour lines represent the coefficient $g(\Omega)$.

Unlike system (1), these equations are written in a frame of reference moving with a group velocity v_{gr}. The terms that represent signal amplification and pump depletion are presented in explicit form. Figure 4 shows simulation results for the amplification of a modulated signal,

$$|A_s(0,t)|^2 = P_{s0}[1 + 0.02\cos(\Omega t)], \qquad (12)$$

at an initial power $P_{s0} = 0.25$ W and $P_{p0} = 25$ W. Physically, this can be brought about, e.g., using a laser with a frequency close to the pump carrier frequency and corresponds to induced MI. We consider a situation with a small group velocity difference, $\delta = 0.05$ ps m^{-1} (see also Fig. 3a). At a modulation frequency $\Omega = 2.1\times10^{12}$ s^{-1}, a modulated signal similar to a pulse train is formed over the length of the amplifier, and the spectrum of the output signal then has the form of harmonics of the modulation frequency that decrease in power. Comparison of the variations in the signal and pump powers (Fig. 4a, dashed lines) to the analytical solution (2), obtained for a continuous signal and pumping, indicates that the pump-to-signal conversion efficiency decreases in the case of strong modulation of the interacting waves, and pumping then changes from continuous to pulsed. Subsequently, when the modulated signal shifts relative to the pump pulses, slight oscillations of the conversion efficiency can be observed.

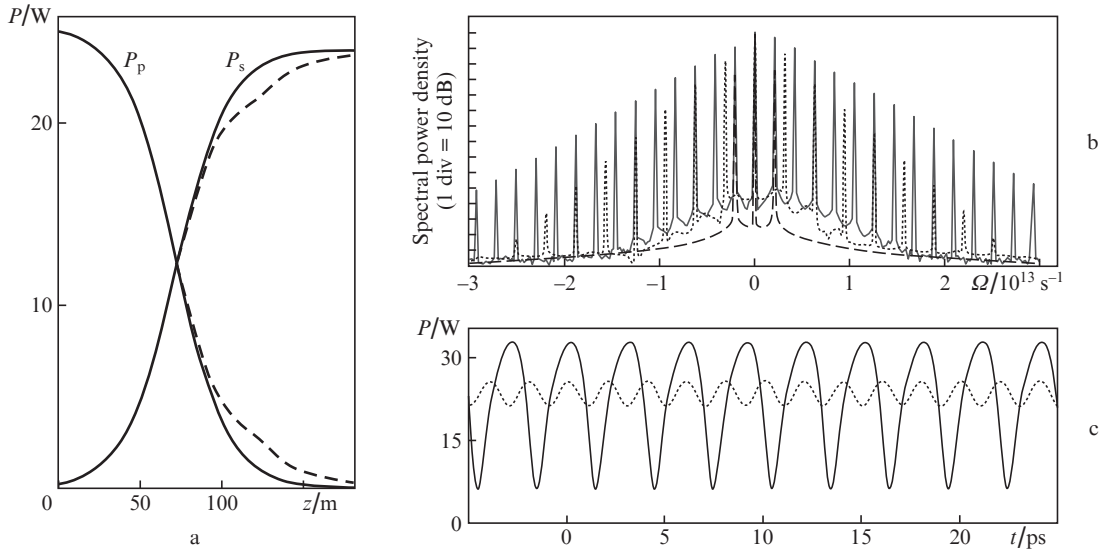

Figure 4. (a) Growth of the signal and pump depletion along the length of an amplifier (the same parameters of the power amplifier as in Fig. 3; the solid lines represent an analytical solution to system (2) and the dashed lines represent numerical simulation of system (11) at a modulation frequency $\Omega_1 = 2.1\times10^{12}$ s^{-1}); (b) numerical simulation results for the spectrum of a signal in a 150-m-long amplifier (the solid line shows the spectrum of the signal at the amplifier output, the long-dashed line shows the spectrum of a modulated signal at the amplifier input at a modulation frequency $\Omega = 2.1\times10^{12}$ s^{-1}, and the short-dashed line shows the spectrum of the output signal at a pump modulation frequency $\Omega = 3.15\times10^{12}$ s^{-1}); (c) numerical simulation results for the output signal of a 150-m-long amplifier (solid line: modulation frequency $\Omega = 2.1\times10^{12}$ s^{-1}; dashed line: $\Omega = 3.15\times10^{12}$ s^{-1}).

Simulation results indicate that, at a modulation frequency $\Omega = 3.15\times10^{12}$ s^{-1}, which roughly corresponds to the maximum in modulation gain (Fig. 3a), no strong modulation of the signal takes place. Thus, the integrated modulation gain coefficient at this frequency is smaller than that at $\Omega = 2.1\times10^{12}$ s^{-1}. In addition, it is worth noting that the results in the previous section were obtained for small harmonic perturbations at one frequency. At the same time, if there is an amplified modulation component, further excitation of its harmonics occurs owing to four-wave mixing. If a harmonic of the modulation frequency also falls within the instability range, it is rapidly amplified through energy transfer from lower harmonics and from the main component at the carrier frequency. This may culminate in the generation of a train of short pulses.

At an appreciable group velocity difference ($\delta = 0.5$ ps m^{-1}), which corresponds to the data in Fig. 3c, simulation results (Fig. 5) confirm that the spectral range of MI decreases and shifts to higher frequencies. Comparison of results obtained for various signal modulation frequencies indicates that the modulation gain varies by more than 25 dB across a 10^{12} s^{-1} band. Note that the spectrum of the modulationally unstable component is asymmetric: because the phase matching condition is fulfilled, the spectrum is shifted to higher frequencies and the modulation 'leads' the signal carrier wave and 'lags' the pump wave.

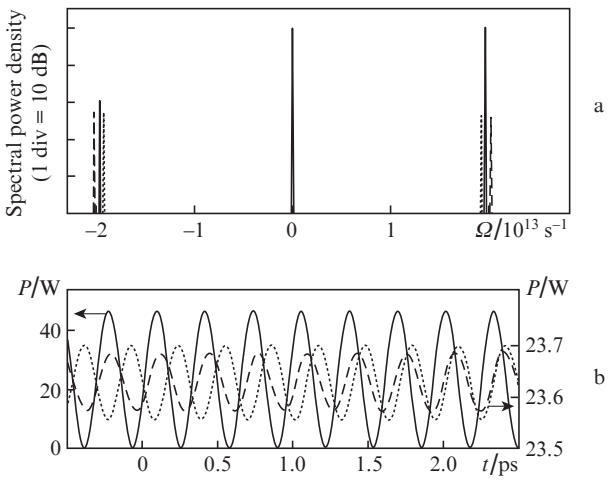

Figure 5. Numerical simulation results (a) for the spectrum of a signal at different modulation frequencies and (b) for the output signal. The same parameters of the amplifier as in Fig. 3; amplifier length, 150 m; $\delta = 0.5$ ps m^{-1}. The short-dashed, solid and long-dashed lines correspond to modulation frequencies $\Omega = (1.925, 1.965$ and $2.015)\times10^{13}$ s^{-1}.

The spectral selectivity of cross modulation interaction can be employed as the basic principle behind the operation of a number of fibre-optic devices, e.g., narrow-band filters. Note again that the parameters used in our computations are typical of real silica fibres in the IR spectral region and that the observed relationships can be used in designing novel fibre-optic devices. In particular, advanced optical fibre fabrication technologies allow one to produce fibres with a tailored group velocity difference at predetermined wavelengths, e.g. by using fibres with a certain refractive index profile [20]. In setting the pump and Raman signal wavelengths in fibre, an amplifier with a predetermined narrow spectrum of its output signal can be designed as 'reference' points. A more detailed description of a fibre with such properties and a related amplifier is beyond the scope of this paper and will be presented in subsequent reports.

5. Cross modulation instability in a Raman fibre laser

Compare the above model for cross modulation instability to available experimental data. It can be seen from the above results that such instability becomes significant only when the signal and pump powers differ little. In optical amplifiers, this situation is only encountered in a limited range of output powers. Such instability shows up more frequently in lasers because, in a transient process resulting in self-consistent, steady-state signal and pump field distributions in the laser cavity, the signal repeatedly passes through a potential instability region, where the signal and pump powers differ little.

Ravet et al. [15] described an experiment aimed at assessing the effect of cross phase modulation on the output spectrum of a cw Raman laser. Figure 6 schematically shows their experimental arrangement. The ring cavity of the Raman fibre laser was closed by a 20% reflectivity fibre Bragg grating. The light propagation direction was controlled by an optical circulator. The laser was pumped in a co- or counterpropagating pump configuration with respect to the signal wave. The essence of the experiment was to compare the output spectra of the laser in the co- and counterpropagating pump configurations, ensured by wavelength-division multiplexers (WDM2 and WDM1).

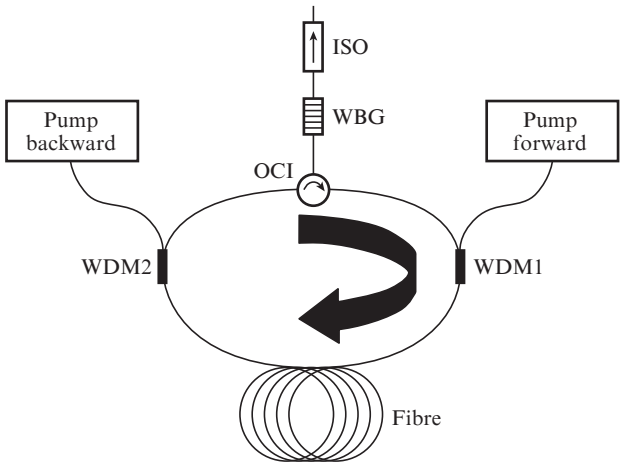

Figure 6. Experimental setup (borrowed from Ravet et al. [15]): (WDM1, WDM2) wavelength-division multiplexers for copropagating and counterpropagating pump schemes, (OCI) optical circulator, (FBG) fibre Bragg grating, (ISO) optical isolator.

Light propagation through the fibre was modelled using system (11). In addition, we analysed reflection from the FBG on each cavity pass using a discrete transformation of the spectrum of a signal wave (the grating was taken to have a Gaussian reflection spectrum):

$$A_s^{out}(\omega) = A_s^{in}(\omega)\sqrt{R}\exp(-\omega^2/\Delta\omega^2),$$

where $R = 0.2$ is the reflectivity of the grating and $\Delta\omega = 10^{12}$ s^{-1} is its reflection bandwidth. The Raman gain bandwidth far exceeds 10^{12} s^{-1}, which allows us to take the Raman gain coefficient

g_R to be frequency-independent. The following experimental parameters were used in simulation: pump and signal wavelengths, 1460 and 1550 nm; normal dispersion in the fibre at these wavelengths $d_p = 0.025$ ps^2 m^{-1} and $d_s = 0.015$ ps^2 m^{-1}; pump power $P_{p0} = 6$ W; Raman gain coefficient $g_R = 0.0022$ W^{-1} m^{-1}; cavity length $L = 200$ m. No other parameters were specified in Ref. [15], so we took typical nonlinearity coefficients of such fibre ($\gamma_p = \gamma_s = 0.0035$ W^{-1} m^{-1}). In the case of the copropagating pump scheme, the group velocity difference δ was taken to be 0.03 ps m^{-1}. To simulate a considerable group velocity difference in the counterpropagating pump scheme, we took $\delta = 30$ ps m^{-1}. The initial signal had the form (12), with a power $P_{s0} = 0.00025$ W and a modulation frequency $\Omega = 1.25\times10^{11}$ s^{-1}, which corresponded to the 50 000th cavity mode. This simplified, schematic model makes it possible to compare simulation results and a theoretical description of MI to experimental data.

After about 50 cavity passes, the simulated spectrum was similar to the experimental spectrum of the Raman laser (Fig. 7). At small δ, the spectrum contained characteristic bands of increased intensity, due to cross modulation instability. At high δ values, corresponding to the counterpropagating pump scheme, there were no such regions.

To interpret the simulation results, we rely on reasoning similar to that above: four-wave mixing increases modulation harmonics. The components of the spectrum for which the phase matching condition is best fulfilled experience higher modulation amplification. At a considerable signal–pump group velocity difference, the modes excited through four-wave mixing are not fed via energy transfer upon MI, and their intensity drops sharply with increasing frequency. Thus, even the simplified model for pump–signal phase interaction in a Raman laser ensures a conceptually accurate description of the laser output spectrum.

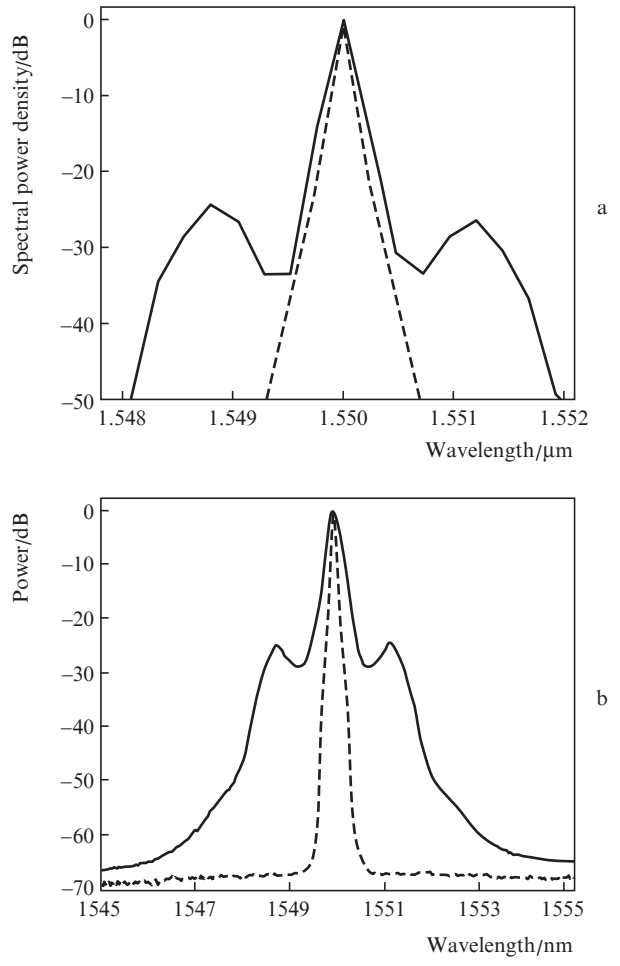

Figure 7. (a) Output spectra obtained by numerical simulation and (b) experimental spectra of a Raman laser [15]. The solid and dashed lines correspond to the copropagating and counterpropagating pump schemes.

Note some possible ways of employing the above general relationships in designing advanced laser sources. In some instances, the use of a modulated copropagating pump configuration may be attractive. Knowing the signal–pump group velocity difference and using (10), one can find the modulation frequency that ensures the maximum gain. This will allow one to realise, using a pump source modulated at this frequency, a laser source with a narrow-band high-frequency modulation capable of generating short pulses at a high repetition rate under certain conditions. A detailed description of such a source will also be presented in subsequent reports.

6. Conclusions

We have studied characteristics of instability resulting from cross phase modulation interaction between signal and pump waves in fibre amplifiers and lasers. We have analysed the dispersion relation for the wave vector of small harmonic perturbations, obtained the modulation gain coefficient as a function of amplifier parameters and examined the dynamics of the unstable frequency range. The present results lead us to the general conclusion that, in describing amplification in optical fibre, one should not ignore phase interaction between the signal and pump wave, especially when their group velocities differ little.

It has been shown that cross modulation instability in amplifiers is most significant when the signal and pump powers differ little and that the spectral range of instability strongly depends on the group velocity difference δ between the signal and pump waves. At low δ values, the modulation gain spectrum has the form of a broad band at low frequencies, which offers the possibility of broadening the spectrum upon the amplification of multiple harmonics of the modulation signal of relatively low frequency and pulse train generation. With increasing δ, the spectral range of instability decreases and shifts to higher frequencies. This behaviour of cross modulation instability can probably be used in practical applications: in designing narrow-band filters and generators of high modulation frequency signals and high repetition rate pulse trains. The present numerical simulations lend support to analytical calculation results and are in qualitative agreement with experimental data.

Acknowledgements. This work was supported by the RF Ministry of Education and Science.

References

1. Agrawal G. *Nonlinear fiber optics* (New York: Springer, 2007).
2. Zakharov V.E., Ostrovsky L.A. *Phys. D*, **238**, 540 (2009).
3. Tai K., Hasegawa A., Tomita A. *Phys. Rev. Lett*., **56**, 135 (1986).
4. Dianov E.M., Mamyshev P.V., Prokhorov A.M., Chernikov S.V. *Opt. Lett*., **14**, 1008 (1989).
5. Rubenchik A.M., Turitsyn S.K., Fedoruk M.P. *Opt. Express*, **18**, 1380 (2010).

6. Korobko D.A., Okhotnikov O.G., Zolotovskii I.O. *J. Opt. Soc. Am. B*, **30**, 2377 (2013).
7. Zolotovskii I.O., Lapin V.A., Sementsov D.I. *Phys. Wave Phenom.*, **21**, 1 (2013).
8. Zolotovskii I.O., Korobko D.A., Lapin V.A. *Kvantovaya Elektron.*, **44**, 42 (2014) [*Quantum Electron.*, **44**, 42 (2014)].
9. Kobtsev S.M., Smirnov S.V. *Opt. Express*, **16**, 7428 (2008).
10. Dudley J.M., Genty G., Dias F., Kibler B., Akhmediev N. *Opt. Express*, **17**, 21497 (2009).
11. Demircan A., Bandelow U. *Opt. Commun.*, **244**, 185 (2005).
12. Agrawal G.P. *Phys. Rev. Lett.*, **59**, 880 (1987).
13. Agrawal G.P., Baldeck P.L., Alfano R.R. *Phys. Rev. A*, **39**, 3406 (1989).
14. Velchev I., Pattnaik R., Toulouse J. *Phys. Rev. Lett.*, **91**, 093905 (2003).
15. Ravet G., Fotiadi A., Blondel M., Mégret P. *Proc. Symposium IEEE/ LEOS Benelux Chapter* (Mons, 2005) p. 201.
16. Toulouse J., Velchev I., Pattnaik R. *Conf. Lasers ans Electrooptics (CLEO 2002)* (Long Beach, CA, USA, 2002) CTh043, p. 535.
17. Zolotovskii I.O., Korobko D.A., Okhotnikov O.G., Sementsov D.I., Sysolyatin A.A., Fotiadi A.A. *Opt. Spektrosk.*, **114**, 286 (2013).
18. Harvey J., Leonhardt R., Coen S., Wong G., Knight J., Wadsworth W., Russell P.St.J. *Opt. Lett.*, **28**, 2225 (2003).
19. Paschotta R. *Encyclopedia of Laser Physics and Technology* (New York: John Wiley & Sons, 2008).
20. Akhmetshin U.G., Bogatyrev V.A., Senatorov A.K., Sysolyatin A.A., Shalygin M.G. *Kvantovaya Elektron.*, **33**, 265 (2003) [*Quantum Electron.*, **33**, 265 (2003)].